CR-39 Detectors Irradiated by Different Radiation Particles and Its Applications

Zhiheng Xu,[a] Erik Ziehm,[b] Matthew Bergschneider,[c] George H. Miley[b]

[a] *Department of Nuclear Science and Engineering, Nanjing University of Aeronautics and Astronautics, Jiangning Dist., Nanjing, Jiangsu 211106, China, xuzhiheng@nuaa.edu.cn*
[b] *Nuclear, Plasma, and Radiological Engineering, University of Illinois at Urbana-Champaign, Urbana, IL 61801, USA*
[c] *Industrial Heat LLC., Champaign, IL 61820*

INTRODUCTION

Radiation track measurement technology has a number of advantageous characteristics: light-weight, small, easy to use, contains simple materials, requires no power supply systems, and often most importantly - inexpensive. The method can be used in high or low dose radiation environments and can permanently save the incident particle's trajectory with high spatial resolution.[1] CR-39, a polyallydiglycol carbonate polymer ($C_{12}H_{18}O_7$), is a type of nuclear track detector used to detect charged particle emission with widespread use in the inertial confinement fusion field.[2, 3] When a radioactive particle passes through the polymer, it produces along its ionization trail a region that is more sensitive to chemical etching than the rest of the bulk. After treatment with an etching solution, tracks remain as holes or pits in the plastic. The size and morphology of the tracks provide information as to what type of particle created the track as well as its energy.[4]

The purpose of this study is presenting the internal response relationship between the characteristic parameters of radiation products and the CR-39 morphology changes, such as the track size distribution and areal fraction quantification. Furthermore, experimental details of particle tracks recorded with CR-39 and its application in Low Energy Nuclear Reaction (LENR) nanoparticle experiments using H_2 or D_2 are stated. Based on the results obtained from the interaction of the CR-39 detectors with known species of radiation, this method can be used to analyze unknown nuclear reaction products - determining whether a site is irradiated and possibly the type and energy of radiation.

MATERIALS AND METHODS

CR-39 is purchased from Track Analysis Ltd. As shown in Fig. 1, the initial size of a single sample is 3.6 cm × 1.5 cm × 0.1 cm. In the actual test, the sample is divided into pieces according to the needs. Three kinds of typical radiation sources were used to compare computational and experimental testing: alpha, beta and gamma. The isotopes were ^{238}U, ^{239}Pu, ^{14}C, ^{133}Ba and ^{60}Co and the specific information is given in Table I.

The interaction between radiating particles and CR-39 were modeled through TRIM and MCNP. The number of total calculated alpha particles is 10,000 in the TRIM calculation. In the Monte Carlo N-Particle Transport Code simulation, the center of the sources and the CR-39 samples was aligned, and the other conditions were consistent with the experiment parameters. The continuous beta energy spectrum was used in the calculation models.

The morphological changes of CR-39 samples before and after irradiation were observed and tested by inverted optical materials microscope (ZEISS Axio Vert.A1)[a]. The optimum etching condition of the comprehensive analysis is 6.5 mol NaOH solution at 70 ± 5 °C for 4-6 hours. The captured images were analyzed by ImageJ and Nano Measurer software. The objects of comparison can be track length and diameter, track size, and image symmetry.

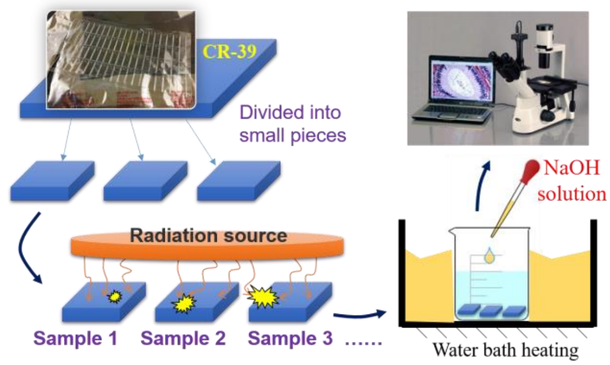

Fig. 1. CR-39 plastic track detectors and treating processes.

TABLE I. Radiation sources information

Source -Types	Half-life (years)	Major energies (keV)	Activity (Bq)
^{239}Pu-α	24131	5156.59 (71%) 5144.3 (17%) 5105.5 (12%)	14.43
^{238}U-α	4.468 x 10^9	4198.3 (79%) 4151.5 (21%)	1960
^{14}C-β	5730	E_{max}-156.48 E_{ave}-49.47	6549
^{133}Ba-γ	10.5	356.017 (62.05%) 80.997 (34.06%) 302.853 (18.33%)	37000
^{60}Co-γ	5.271	1173.2 (50%) 1332.5 (50%)	37000

RESULTS

Different Kinds of Radiation

Fig. 2 shows the accumulated energy distribution in the CR-39. The simulation results reflect that the penetration depth of alpha and beta particles in the CR-39 track detector is much smaller than its thickness (0.1 cm). This means that most of the radiation sources' energy is deposited in the detector. The result of gamma particles is just the opposite. At the same time, the particle penetration depth from U-238 is less than that of Pu-239. The specific results of alpha particles incident on CR-39 with corresponding energy spectra to that of U-238 and Pu-239 was computed with TRIM and are provided in Table II.

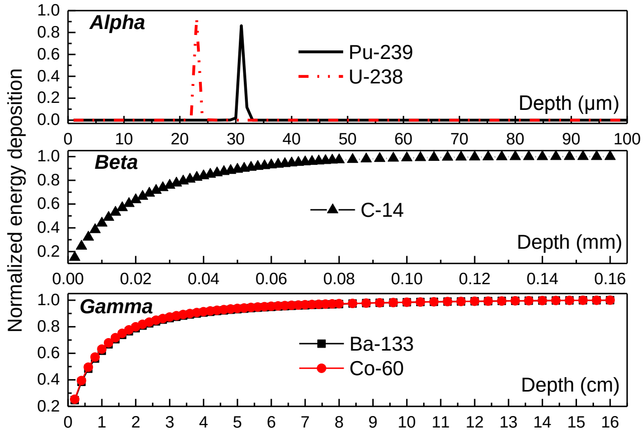

Fig. 2. Relationship between particle energy deposition and CR-39 thickness.

TABLE II. Alpha particles interact with CR-39 using TRIM

Source	Average Range (μm)	Lateral Range (μm)	Radial Range (μm)
^{239}Pu	30.65 ± 0.38	0.39 ± 0.58	0.61 ± 0.52
^{238}U	22.62 ± 0.22	0.32 ± 0.48	0.50 ± 0.42

The effect of alpha, beta, and gamma particles on the morphology of CR-39 detectors in the same irradiation time (58.5 hours) were studied. The results of different kinds of radiation particles deposited on the CR-39 plastic track detectors are provided in Fig. 3. The most impressive change is the detectors exposed to alpha sources. There are many small tracks. The sizes are 130-230 μm and 100-150 μm for Pu-239 and U-238, respectively. The tracks are denser for U-238. Some small tracks can be seen from beta, gamma sources, and blank control. However, the beta and gamma tracks are almost indistinguishable from the blank control. Therefore, this CR-39 is relatively more sensitive to the heavy charged particles than electrons and gamma rays.

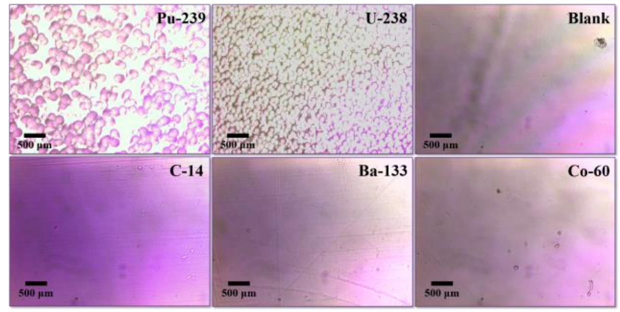

Fig. 3. ×20 magnification for CR-39 processed in different types of radiation, etched 6 hours.

Different Fluence and Energy of Alpha Particles

The morphologies of CR-39 samples under different alpha sources (U-238 and Pu-239) with the same fluence were compared. Fig. 4 shows the correlation between irradiation time, particle energy, and track size and density. CR-39 detectors irradiated with both alpha sources showed an increase in track density with increasing irradiation time. Overall, the track diameter decreased gradually with the irradiation time, except for the CR-39 irradiated 79.5 seconds by U-238. Under the same alpha particle fluence irradiation, the track density of Pu-239 is significantly greater than that of U-238. The experimental results are in good agreement with the range calculated by theoretical simulation. At the same time, in the alpha particle irradiation experiments, shortening the etching time of the CR-39 can lead to more conical bubbles.

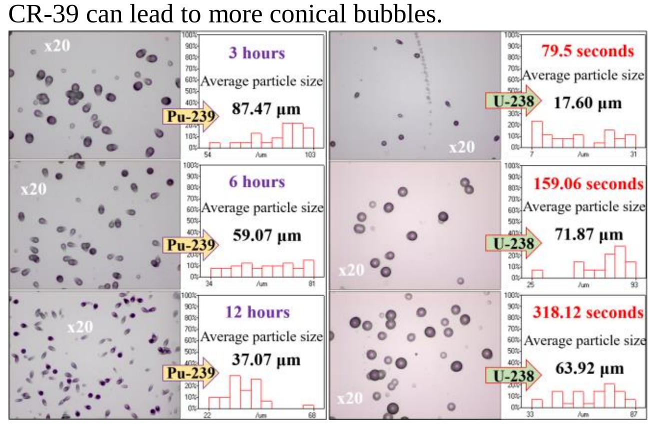

Fig. 4. ×20 magnification for CR-39 under different fluences of alpha particle irradiation, etched 4 hours.

Fig. 5 shows the morphological changes of the CR-39 samples partially covered with different barrier materials (Copper, Aluminum, and Mylar) under the same U-238 irradiation source. Different materials have varying resistance to alpha particles with the stopping power in order from strongest to weakest: copper, aluminum, and Mylar. After passing through different barrier materials, the flux and the amount of alpha particles are attenuated. The clarity of the boundary can also illustrate this point from the images. As the irradiation time increases, the tracks become denser. In the area covered by the material, the track size is relatively stable with minimal fluctuations resulting from alpha particle irradiation time and the blocking material. From the average size of the tracks, the density is slightly more concentrated as the irradiation time is lengthened.

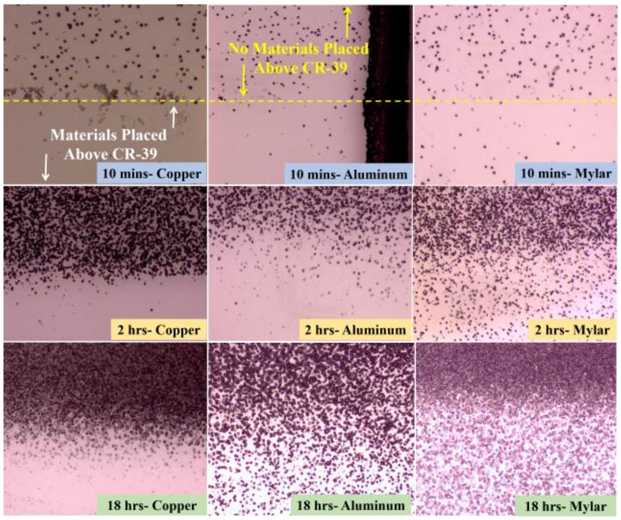

Fig. 5. ×5 magnification for CR-39 under U-238 irradiation with different block materials.

Application of CR-39 in the LENR nanoparticle experiments

This radiation detection method is applied to other occasions where low dose radiation needs to be monitored in environments hostile to traditional detectors due to temperature swings, high-vacuum conditions, or electrical interference. Such an application was in the pursuit of investigating LENR nanoparticle experiments. According to the change of topography, we can analyze the possible radiation phenomena in the process of low-energy nuclear reaction. A comparative trial was initially carried out: CR-39 exposed to D_2 or H_2 with no nanoparticles (set as D0 and H0), and embedded in nanoparticles exposed to D_2 or H_2. The nanoparticle experiments were pressurized at increasing intervals of three absorption-desorption cycles. That is for the first set (D1 or H1), the nanoparticles were pressurized three times before imaging the CR-39, second set - six times, third set - nine times, etc. Each set was completely self-contained with the nanoparticles and CR-39 never being removed until the desired number of runs was attained. In general, as the number of cycles increases, the morphology changes of the CR-39 are more obvious, and some clear bubbles become apparent.

For the CR-39 embedded in nanoparticles and exposed to H_2 or D_2, the particle tracks can be seen in Fig. 6. Due to the relationship between the size of the experimental chamber and the size of the field of view under the microscope, the samples were divided into different regions. Sections along the CR-39 were labeled – up, center, and down – and display varying bubble sizes and densities. Some bubble trajectories appear similar to those produced from alpha particle irradiation. This shows the feasibility of the CR-39 for radiation detection in the LENR nanoparticle experiments.

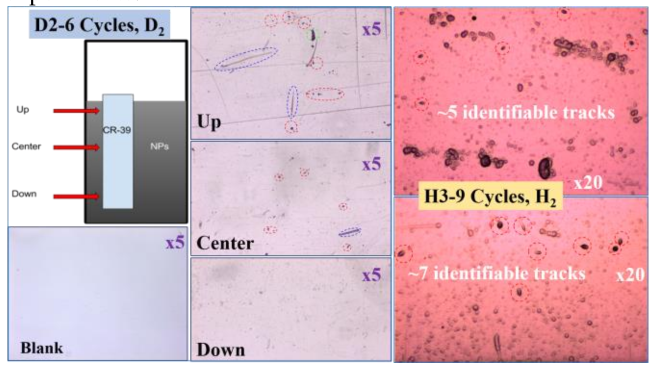

Fig. 6. Close-ups of CR-39 embedded in nanoparticles.

CONCLUSION

The objective of this study was to detect and analyze low-intensity radioactive sources using CR-39. The results showed that alpha particles produced the most tracks while gammas produced the least as is expected due to interaction cross-sections. Barrier materials were used to attenuate alpha energies and to observe the resulting augmented track characteristics. The results showed little change in track profiles and only the density of tracks decreased with increasing barrier stopping power. The applications of radiation detection with CR-39 embedded in nanoparticles and exposed to H_2 or D_2 were also discussed which displays CR-39's versatility being simpler, less expensive, and with a higher detection efficiency than traditional detectors.

ACKNOWLEDGMENTS

The authors would like to acknowledge and thank the Frederick Seitz Materials Research Laboratory Central Research Facilities, University of Illinois for providing laboratory equipment for these experiments.

REFERENCES

1. A. S. Roussetski, "Application of CR-39 plastic track detector for detection of DD and DT-reaction products in cold fusion experiments" *Condens. Matter Nucl. Sci. – Proc. ICCF-8*, Lerici (La Spezia), Italy, May 21–26, 2000, Conference Proceedings- Italian Physical Society (2000).
2. A. S. Roussetski, et al., "Correct identification of energetic alpha and proton tracks in experiments on CR-39 charged particle detection during hydrogen desorption from Pd/PdO: Hx heterostructure", *Condens. Matter Nucl. Sci. – Proc. ICCF-10*, **12**, 304 (2005).
3. L. Kowalski, "Comment on "The use of CR-39 in Pd/D co-deposition experiments" by PA Mosier-Boss, S. Szpak, FE Gordon and LPG Forsley Interpreting SPAWAR-type dominant pits", *The Eu. Phys. J. Appl. Phys.*, **44**, 3 (2008).
4. Pamela A. Mosier-Boss, Lawrence P.G. Forsley, Patrick K. McDaniel, "Investigation of nano-nuclear reactions in condensed matter", Defense Threat Reduction Agency (2016).